Abdullah M. Wali
Mohammed Y. Khdiar

Department of Biology,
College of Education,
Al Iraqia University,
Baghdad, IRAQ

Effect of Precursor Concentration on Structural Characteristics of Titanium Dioxide Nanopowders Synthesized by Green Method

In this work, titanium dioxide nanopowders were synthesized by an eco-friendly green method. The structural characteristics of the synthesized nanopowders were determined, analyzed and compared to introduce their dependency on the precursor concentration. It was found that the synthesized nanopowders show polycrystalline structures with a reasonable dependency on the concentration of the precursor of the TiO_2 (i.e., titanium isopropoxide). Also, the minimum particle size was found to increase with increasing the concentration of the precursor. Higher concentration of the precursor results in much more stoichiometric compound. The lowest concentration (0.5 mL) has resulted in higher surface roughness. The synthesized nanopowders will be employed in biological and agricultural applications to make use of the photocatalytic activity of TiO_2.

Keywords: Titanium dioxide; Nanopowders; Green synthesis, Reduction method
Received: 20 March 2025; **Revised:** 28 April 2025; **Accepted:** 04 May 2025

1. Introduction

Eco-friendly nanomaterial manufacturing methods, known as green technologies, offer numerous advantages compared to other methods and techniques. They are characterized by low cost, minimal requirements, high availability, and rapid production. They also can be applied near the field, saving time, effort, storage, and transportation [1-4].

One of the most commonly used green methods for producing nanomaterials is the chemical reduction of nanomaterials from their chemical precursors using plant extracts [5]. This method can produce a variety of nanomaterials depending on the available plant-based components in the surrounding environment [6]. It offers several advantages that other methods cannot provide, primarily the absence of harmful emissions and the ability to utilize plant residues by converting them into materials that can be easily returned to the soil as stimulants and enhancers [7,8]. Also, it does not require complex or costly procedures and ensures the abundant production of nanomaterials, making it a viable source for applications that demand relatively large quantities of the desired nanomaterials [9-11].

The interest in using nanomaterials in biological and agricultural applications is continuously increasing due to the unique properties and characteristics these materials exhibit, which cannot be offered by conventional chemical fertilizers and growth stimulants [12-14]. Titanium dioxide stands out among these materials, especially when prepared in the form of a nanopowder, as it benefits from the synergistic effect of the quantum size of the nanoparticles and the photocatalytic activity that this material possesses [15,16].

Titanium dioxide nanoparticles (TiO_2 NPs) have gained increasing attention in agricultural research due to their nanoscale dimensions and favorable physicochemical properties [17-20]. These include a high surface area-to-volume ratio, strong ultraviolet (UV) absorption, high photocatalytic activity, and exceptional chemical stability [21-24]. These features make TiO_2 NPs highly suitable for enhancing plant physiological functions and protecting crops from various biotic and abiotic stresses [25]. The agricultural behavior and efficacy of TiO_2 NPs are determined by properties such as their crystalline phase (anatase vs. rutile), particle size, surface charge, and tendency to aggregate. The anatase phase, in particular, exhibits superior photocatalytic activity, enabling more efficient interaction with light and promotion of photosynthesis [26-28]. However, it can also present phytotoxicity risks at elevated concentrations [25]. TiO_2 NPs may interact with plant surfaces through foliar application or enter the root zone via the soil, where environmental factors like pH, moisture, and microbial communities influence their mobility and bioavailability [29,30]. One of the most recognized benefits of TiO_2 NPs in agriculture is their ability to enhance photosynthetic performance. These nanoparticles have been shown to promote chlorophyll biosynthesis, optimize light absorption, and stimulate photosynthetic enzyme activity [31]. Their light-scattering and UV-blocking properties help reduce photodamage to chloroplasts and improve photon use efficiency [25]. For instance, in *Vetiveria zizanioides* (vetiver grass), TiO_2 NPs significantly enhanced physiological parameters such as net photosynthetic rate, stomatal conductance, and transpiration rate [32]. TiO_2 NPs are known to exhibit hormetic effects—wherein low concentrations stimulate plant growth and metabolic functions, while higher doses induce inhibitory or toxic effects. At optimal doses, they

promote root elongation, shoot growth, and resilience to environmental stresses. In contrast, excessive exposure may lead to oxidative stress, chlorosis, and disruption of DNA integrity in plant cells [25]. This biphasic response underlines the importance of dosage optimization for the safe and beneficial use of TiO_2 NPs in agricultural applications [33,34].

During the last three decades, several methods and techniques, such as sol-gel, pulsed-laser deposition, chemical bath deposition, reactive sputtering, solvothermal and chemical reduction, were used to prepare TiO_2 nanoparticles with highly controlled characteristics to serve certain applications [35-38]. Each method or technique may have advantages over the other ones, however, the solvothermal chemical method was selected in this work due to the advantages mentioned before [39,41].

Titanium dioxide nanopowders were prepared by the chemical reduction of titanium isopropoxide as a precursor using aqueous solution of banana peels. The structural characteristics of the prepared nanopowders were determined and analyzed to introduce the effect of precursor concentration on these characteristics.

2. Experimental Work

Figure (1) shows schematically the experimental setup used for the preparation of TiO_2 nanopowders. Banana peels were used as a resource for plant-derived titanium, while titanium isopropoxide ($C_{12}H_{28}O_4Ti$) served as the precursor material. Fresh, unripe bananas were obtained from the local market, and their peels were cut into small pieces, washed three times with deionized distilled water (DDW) to remove any impurities, and dried using absorbent paper. Then, 80 g of the dried peels were weighed and placed in a beaker containing 150 mL of DDW. The mixture was heated up to its boiling point (100°C) and maintained at this point for 20 minutes. After boiling, the mixture was filtered using Whatman® #1 filter paper to remove solid residues.

In a separate flask, an aqueous solution was prepared by dissolving certain volume (0.5, 1, and 2 mL) of $C_{12}H_{28}O_4Ti$ in 10 mL of DDW. This solution was heated up to 40°C on a hotplate stirrer for 10 minutes with continuous stirring to ensure complete dissolution and homogeneity. The heating step was then turned off, but stirring was continued while immediately preceding to the next step.

The banana peel extract was gradually added to the $C_{12}H_{28}O_4Ti$ solution in 5 mL increments while stirring continuously for one hour to promote nanoparticle formation. The chemical reaction of the precursor with the aqueous solution to produce titanium dioxide as a solid nanopowder and isopropyl alcohol is shown as

$$C_{12}H_{28}O_4Ti\ (l) + 2H_2O\ (l) \rightarrow TiO_2\ (s) + 4(CH_3)_2CHOH\ (l)$$

The resulting mixture was then filtered using Whatman® #1 filter paper to collect the synthesized nanopowder. This nanopowder was thoroughly washed with DDW to remove any remaining impurities from the previous steps. Subsequently, the collected nanopowder was subjected to controlled heating until it turned dark grey. Finally, the material underwent a potassium hydroxide (KOH) treatment to enhance purity and eliminate any residual organic matter.

The synthesized samples were characterized by x-ray diffraction (XRD) using PanAnalytical ARIES x-ray diffractometer, field-emission scanning electron microscopy (FE-SEM), energy-dispersive x-ray spectroscopy (EDS) using an FEI Inspect^{TM} 50 FE-SEM instrument, and nanosurf atomic force microscopy (AFM).

Fig. (1) Schematic diagram of the experimental setup used in this work

3. Results and Discussion

Figure (1) shows the XRD patterns of the synthesized nanopowder samples using different concentrations of the precursor ($C_{12}H_{28}O_4Ti$). For lower concentrations (0.5 and 1 mL), the prepared TiO_2 material contains anatase phase only, while the higher concentration (2 mL) has resulted in the appearance of four diffraction peaks belonging to the rutile phase. This is attributed to the increase in enthalpy of the reaction with increasing the concentration of precursor, which lead to induce the phase transformation from anatase to rutile. Despite that the transformation temperature is determined at 600°C for bulk structures of TiO_2, at the nanoscale, reasonably lower temperatures may induce this phase

transformation as the surface-to-volume of the prepared material is increased by three orders of magnitude when the dimensions are reduced from micro to nanoscale [42].

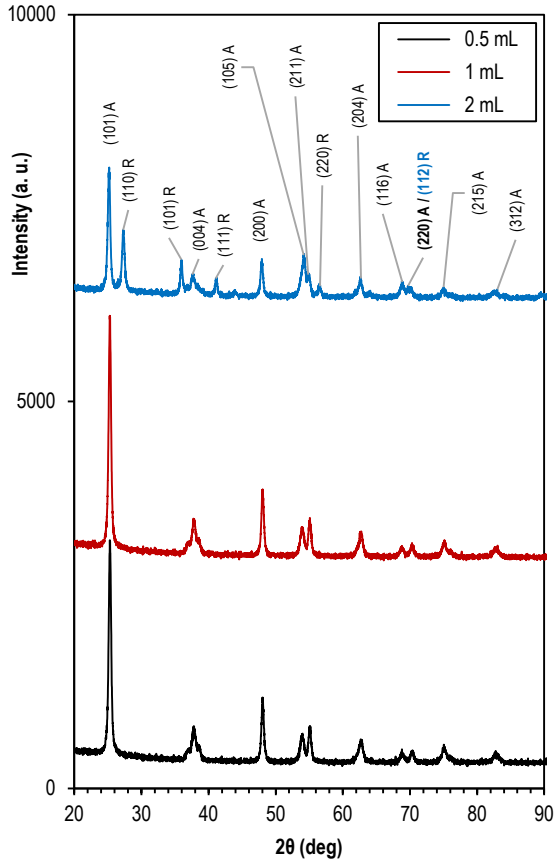

Fig. (1) XRD patterns of the synthesized nanopowders using different concentrations of the $C_{12}H_{28}O_4Ti$ precursor

Table (1) shows the crystalline structural parameters of the prepared samples obtained from XRD results. It is clear that the average crystallite size increases with increasing the concertation of the precursor with a featured appearance of the rutile distinct peak at 27.28°. Another important finding related to the increase of precursor concentration is the observed decrease in the microstrain of the prepared sample. Such decrease may result in a decrease in light absorption by the prepared TiO_2 sample [43]. Therefore, the structural characteristics of the prepared nanomaterial should be carefully analyzed and controlled due to the correlation to the spectroscopic characteristics, which are required to be optimized in applications based on photocatalytic activity of the prepared material.

Figure (2) shows the FE-SEM images of the synthesized nanopowder samples using different concentrations of the precursor ($C_{12}H_{28}O_4Ti$). For all concentrations, the prepared samples show spherical particles with reasonable agglomerated regions. However, the minimum particle size was found to increase with increasing the concentration of the precursor (Fig. 3). This is attributed to the role of higher concentration to produce much more TiO_2 nanoparticles during the same period time taken by the reduction reaction to complete. Therefore, the probability of the grains to grow and form larger particles is increased. The increase in the minimum particle size is about 12% as the precursor concertation is increased from 0.5 to 2 mL, and this value is not sufficiently effective in changing the photocatalytic activity of the prepared sample.

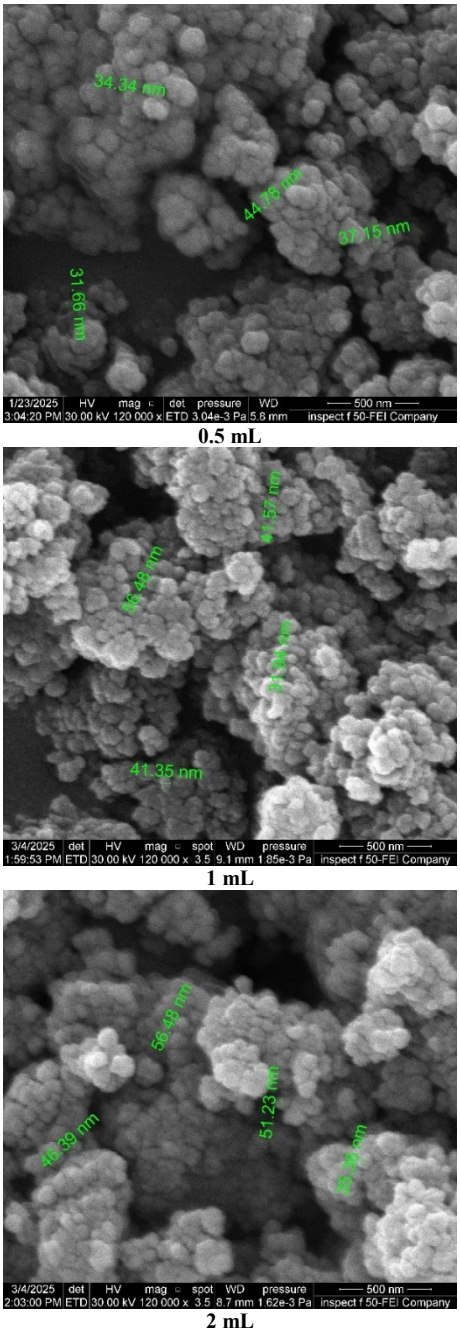

Fig. (2) FE-SEM images of the synthesized nanopowders using different concentrations of the $C_{12}H_{28}O_4Ti$ precursor

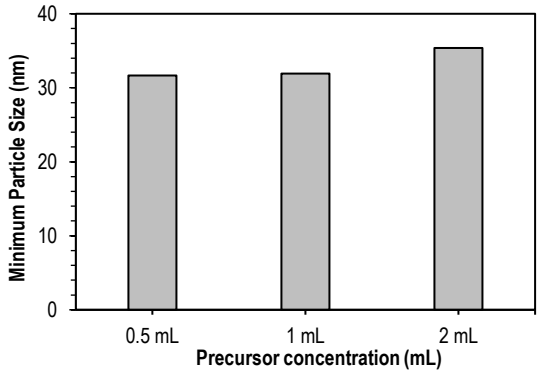

Fig. (3) Variation of minimum particle size of the nanopowder samples with concentration of the $C_{12}H_{28}O_4Ti$ precursor

It was confirmed that the stoichiometry of the TiO_2 materials may affect their spectroscopic characteristics, which are very sensitive to the elemental structure of the material. Therefore, the elemental analysis of the prepared samples is presented in EDS spectra shown in Fig. (4). All samples showed high structural purity as no peaks belonging to elements other than titanium, oxygen and carbon were found. Carbon is originated from two sources, the residual isopropyl alcohol (which is a result of the reduction reaction) and the mounting method used in EDS test.

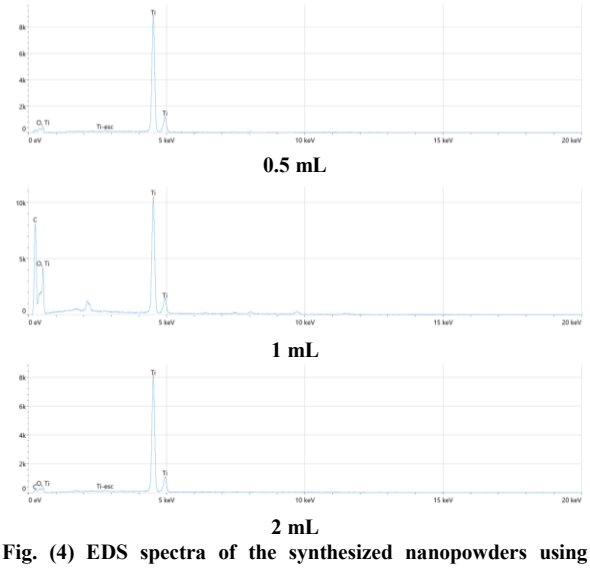

Fig. (4) EDS spectra of the synthesized nanopowders using different concentrations of the $C_{12}H_{28}O_4Ti$ precursor

Figure (5) indicates the variation of the elemental contents in the prepared samples with the precursor concentration. The ratio of [O]/[Ti] represents the indicator of the sample stoichiometry and the sample prepared using the highest concentration (2 mL) showed a [O]/[Ti] ratio of 1.9, which is very close to the typical value of 2. This result is ascribed to the role of higher concentration in providing more titanium atoms for the reaction to form titanium dioxide molecules.

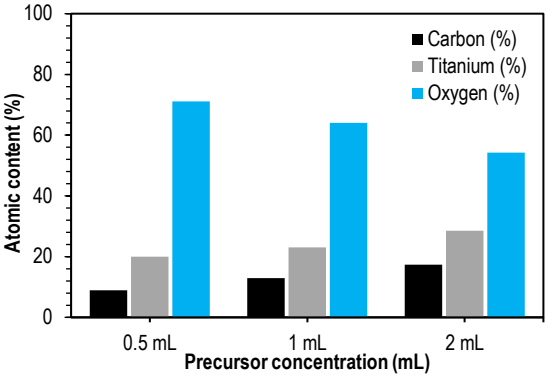

Fig. (5) Variation of atomic contents of carbon, titanium and oxygen in the nanopowder samples with concentration of the $C_{12}H_{28}O_4Ti$ precursor

Figure (6) shows the 2D AFM images of the synthesized nanopowder samples using different concentrations of the precursor ($C_{12}H_{28}O_4Ti$). The surface roughness of the prepared material is very advantageous for the applications based on the radiation-matter interaction as the high surface roughness provide larger surface for such interaction and hence higher opportunity for the aimed events. Apparently, the lowest concentration (0.5 mL) has resulted in higher surface roughness due to the lowest particle size of the nanostructures within this sample.

The surface roughness of a nanomaterial can significantly influence its photocatalytic activity as a rougher surface provides a higher surface area, offering more active sites for photocatalytic reactions. This enhances the interaction between the catalyst, reactants, and light, leading to improved reaction rates. Also, surface roughness can enhance light trapping through increased light scattering and reflection. This allows for more effective absorption of light, particularly in materials like titanium dioxide (TiO_2) that rely on UV or visible light for photocatalysis. Additionally, a rough surface often introduces more surface defects or irregularities that can act as charge carrier traps. While some defects may facilitate charge separation and prevent recombination, excessive surface defects might lead to charge recombination, reducing photocatalytic efficiency. Nanomaterials with rough surfaces typically exhibit improved mass transfer of reactants and products. The porous or uneven texture can facilitate better diffusion, accelerating reaction rates. Finally, surface roughness can increase the hydrophilicity of nanomaterials, enhancing the adsorption of water and pollutants. Improved adsorption promotes effective photocatalytic degradation of contaminants. Consequently, optimizing the surface roughness to balance increased

surface area and minimized charge recombination is crucial for maximizing photocatalytic performance.

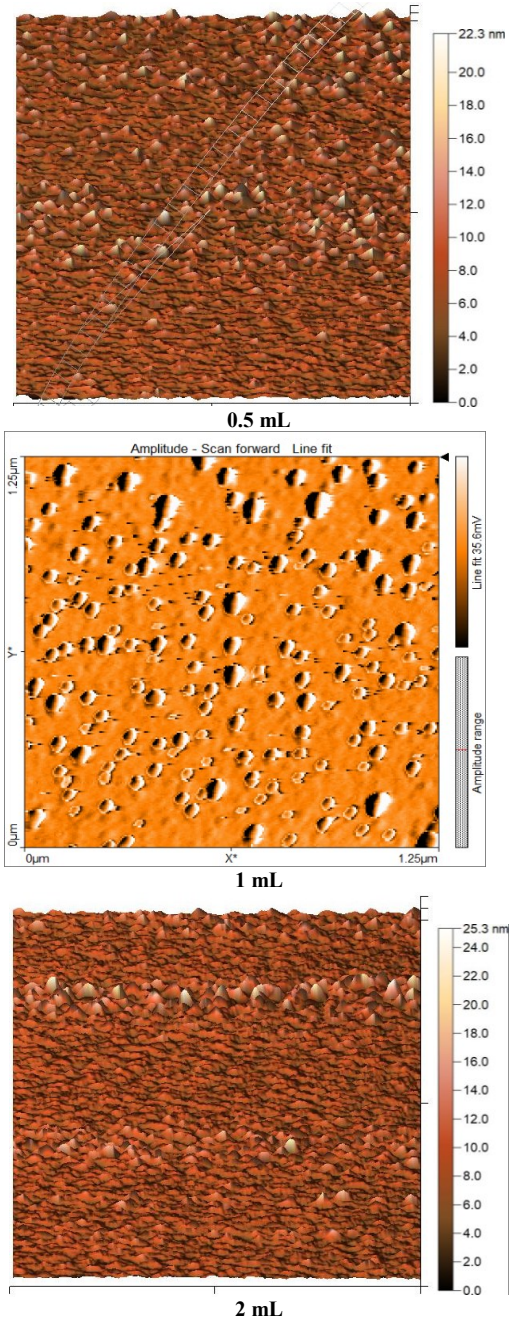

Fig. (6) FE-SEM images of the synthesized nanopowders using different concentrations of the $C_{12}H_{28}O_4Ti$ precursor

4. Conclusion

In concluding remarks, TiO_2 nanopowders were successfully synthesized by an eco-friendly green synthesis method. The synthesized nanopowders show polycrystalline structures with a reasonable dependency on the concentration of the precursor of the TiO_2 (i.e., titanium isopropoxide). As this concentration is increased, the rutile phase of TiO_2 has appeared much more apparently than lower concentrations. Also, the minimum particle size was found to increase with increasing the concentration of the precursor due to the role of higher concentration to produce much more TiO_2 nanoparticles during the same period time taken by the reduction reaction to complete. Higher concentration of the precursor results in much more stoichiometric compound due to the role of higher concentration in providing more titanium atoms for the reaction to form titanium dioxide molecules. Finally, the lowest concentration (0.5 mL) has resulted in higher surface roughness due to the lowest particle size of the nanostructures within this sample. The synthesized nanopowders will be employed in biological and agricultural applications to make use of the photocatalytic activity of TiO_2.

References

[1] N. Baig, I. Kammakakam and W. Falath, "Nanomaterials: A review of synthesis methods, properties, recent progress, and challenges", *Mater. Adv.*, 2(6) (2021) 1821-1871.

[2] H.H.M. Darweesh, "Nanomaterials: classification and properties - Part I", *Nanosci.*, 1(1) (2018) 1-11.

[3] S.S. Salem et al., "A comprehensive review of nanomaterials: Types, synthesis, characterization, and applications", *Biointerface Res. Appl. Chem*, 13(1) (2022) 41.

[4] M. Huston et al., "Green synthesis of nanomaterials", *Nanomater.*, 11(8) (2021) 2130.

[5] O.V Salata, "Applications of nanoparticles in biology and medicine," *J. Nanobiotech.*, 2(1) (2004) 1-6.

[6] A. Mageswari et al., "Nanomaterials: classification, biological synthesis and characterization", *Nanosci. Food Agric.,* 3 (2016) 31-71.

[7] M. Tomás-Gamasa and J.L. Mascareñas, "TiO_2-Based Photocatalysis at the Interface with Biology and Biomedicine", *Chem. Bio. Chem.*, 21(3) (2020) 294-309.

[8] S. Hussain et al., "Green Synthesis of TiO_2 Nanoparticle in *Morus nigra* Leaves; Characterization and Biological Potential", *Pol. J. Environ. Stud.*, 33(3) (2024) 2707-2714.

[9] M. Aravind, M. Amalanathan and M. Sony Michael Mary, "Synthesis of TiO_2 nanoparticles by chemical and green synthesis methods and their multifaceted properties", *SN Appl. Sci.*, 3 (2021) 409.

[10] Y. Astiawanti, N. Faaizatunnisa and M. Munasir, "Green synthesis of TiO_2 (anastase) nanoparticles using *aloe vera* extract as a reducing agent for photocatalytic material", *J. Phys.: Conf. Ser.*, 2900 (2024) 012005.

[11] R. Chandoliya et al., "Titanium Dioxide Nanoparticle: A Comprehensive Review on Synthesis, Applications and Toxicity", *MDPI*

plants, 13 (2024) 2964.
[12] A. Ghareeb et al., "Unlocking the potential of titanium dioxide nanoparticles: an insight into green synthesis, optimizations, characterizations, and multifunctional applications", *Microbio. Cell Fact.*, 23 (2024) 341.
[13] N.M. Alabdallah et al., "Physical, chemical, and biological routes of synthetic titanium dioxide nanoparticles and their crucial role in temperature stress tolerance in plants", *Heliyon*, 10(4) (2024) e26537.
[14] M.-A. Gatou et al., "Photocatalytic TiO_2-Based Nanostructures as a Promising Material for Diverse Environmental Applications: A Review", *Reactions*, 5(1) (2024) 135-194.
[15] O.A. Hammadi, F.J. Kadhim and E.A. Al-Oubidy, "Photocatalytic Activity of Nitrogen-Doped Titanium Dioxide Nanostructures Synthesized by DC Reactive Magnetron Sputtering Technique", *Nonl. Opt. Quantum Opt.*, 51(1-2) (2019) 67-78.
[16] Y.A. Shaban et al., "Photocatalytic degradation of phenol in natural seawater using visible light active carbon modified (CM)-n-TiO_2 nanoparticles under UV light and natural sunlight illuminations", *Chemosphere*, 91(3) (2013) 307-313.
[17] M. Shah et al., "Green synthesis of metallic nanoparticles via biological entities", *Materials (Basel)*, 8(11) (2015) 7278-7308.
[18] K.B. Narayanan and N. Sakthivel, "Biological synthesis of metal nanoparticles by microbes", *Adv. Colloid Interface Sci.*, 156(1-2) (2010) 1-13.
[19] E.A. Al-Oubidy and F.J. Al-Maliki, "Effect of Gas Mixing Ratio on Energy Band Gap of Mixed-Phase Titanium Dioxide Nanostructures Prepared by Reactive Magnetron Sputtering Technique", *Iraqi J. Appl. Phys.*, 14(4) (2018) 19-23.
[20] Z.H. Zaidan, K.H. Mahmood and O.A. Hammadi, "Using Banana Peels for Green Synthesis of Mixed-Phase Titanium Dioxide Nanopowders", *Iraqi J. Appl. Phys.*, 18(4) (2022) 27-30
[21] K. Vijayaraghavan and T. Ashokkumar, "Plant-mediated biosynthesis of metallic nanoparticles: A review of literature, factors affecting synthesis, characterization techniques and applications", *J. Environ. Chem. Eng.*, 5(5) (2017) 4866-4883.
[22] F.J. Al-Maliki and E.A. Al-Oubidy, "Effect of gas mixing ratio on structural characteristics of titanium dioxide nanostructures synthesized by DC reactive magnetron sputtering", *Physica B: Cond. Matter*, 555 (2019) 18-20.
[23] N.M. Noah and P.M. Ndangili, "Green synthesis of nanomaterials from sustainable materials for biosensors and drug delivery", *Sensors Int.*, 3 (2022) 100166.
[24] F.J. Al-Maliki, O.A. Hammadi and E.A. Al-Oubidy, "Optimization of Rutile/Anatase Ratio in Titanium Dioxide Nanostructures prepared by DC Magnetron Sputtering Technique", Iraqi J. Sci., 60(special issue) (2019) 91-98.
[25] A. Trela-Makowej, A. Orzechowska and R. Szymańska, "Less is more: The hormetic effect of titanium dioxide nanoparticles on plants", *Sci. Total Environ.*, 910 (2024) 168669.
[26] Z.H. Zaidan, O.A. Hammadi and K.H. Mahmood, "Effect of Structural Phase on Photocatalytic Activity of Titanium Dioxide Nanoparticles", *Iraqi J. Appl. Phys.*, 19(3A) (2023) 55-58.
[27] E.A. Al-Oubidy and F.J. Al-Maliki, "Photocatalytic activity of anatase titanium dioxide nanostructures prepared by reactive magnetron sputtering technique", *Opt. Quantum Electron.*, 51(1-2) (2019) 23.
[28] F.J. Al-Maliki et al., "Enhanced photocatalytic activity of Ag-doped TiO_2 nanoparticles synthesized by DC Reactive Magnetron Co-Sputtering Technique", *Opt. Quantum Electron.*, 52 (2020) 188.
[29] Y. Bouachiba et al., "Structural and optical properties of TiO_2 thin films grown by sol-gel dip coating process", *Mater. Sci.*, 32 (2014) 1-6.
[30] I. Hussain et al., "Green synthesis of nanoparticles and its potential application", *Biotechnol. Lett.*, 38 (2016) 545-560.
[31] L. Zainab et al., "Impact of titanium dioxide nanoparticles on agricultural crops performance: A review of efficacy and mechanisms", *Futur. Biotech.*, 4(4) (2024) 12–20.
[32] R. Shabbir et al., "Potential of titanium dioxide nanoparticles to improve growth and photosynthetic performance in Vetiveria zizanioides", *Fresenius Enviro. Bull.*, 28(5) (2019) 3734–3742.
[33] A.L. Stepanov, "Titanium dioxide photocatalysis: fundamentals and applications—A review", in **"Photocatalysis - Fundamentals and Perspectives"**, M. Putz (ed.), Springer (2013), pp. 1-28
[34] A. Vatankhah et al., "Plants exposed to titanium dioxide nanoparticles acquired contrasting photosynthetic and morphological strategies depending on the growing light intensity: A case study in radish", *Sci. Rep.*, 13 (2023) 5873.
[35] O.A. Hammadi, "Effects of Extraction Parameters on Particle Size of Titanium Dioxide Nanopowders Prepared by Physical Vapor Deposition Technique", *Plasmonics*, 15(6) (2020) 1747-1754.
[36] R.A.H. Hassan and F.T. Ibrahim, "Preparation and Characterization of Anatase Titanium Dioxide Nanostructures as Smart and Self-Cleaned Surfaces", *Iraqi J. Appl. Phys.*, 16(4) (2020) 13-18.

[37] F.J. Kadhim, O.A. Hammadi and N.H. Mutesher, "Photocatalytic activity of TiO_2/SiO_2 nanocomposites synthesized by reactive magnetron sputtering technique", *J. Nanophot.*, 16(2) (2022) 026005 DOI: 10.1117/1.JNP.16.026005
[38] M.A. Hameed, S.H. Faisal, R.H. Turki, "Characterization of Multilayer Highly-Pure Metal Oxide Structures Prepared by DC Reactive Magnetron Sputtering Technique", *Iraqi J. Appl. Phys.*, 16(4) (2020) 25-30
[39] Z.H. Zaidan, O.A. Hammadi and K.H. Mahmood, "Effect of Preparation Method on Crystalline Structure of Titanium Dioxide Nanoparticles", *Iraqi J. Appl. Phys. Lett*., 6(2) (2023) 11-14.
[40] Z.H. Zaidan, O.A. Hammadi and K.H. Mahmood, "Plant-Extracted Preparation of Crystalline Titanium Dioxide Nanoparticles", *Iraqi J. Appl. Phys. Lett*., 6(4) (2023) 23-26.
[41] D.M. Challoob, M.Y. Khdiar and O.A. Hammadi, "Highly-Pure Titanium Dioxide nanopowders Synthesized by EcoFriendly Solvothermal Method", *Iraqi J. Appl. Phys.,* 20(2B) (2024) 381-386.
[42] H.E. Swanson, **"Standard X-ray Diffraction Powder Patterns**", vol. 25, US Department of Commerce, National Bureau of Standards (1953).
[43] K.I John et al., "Unravelling the effect of crystal dislocation density and microstrain of titanium dioxide nanoparticles on tetracycline removal performance", *Chem. Phys. Lett.*, 776 (2021) 138725.

Table (1) Crystalline structural parameters obtained from XRD results

0.5 mL				
2θ (deg)	**d-spacing (Å)**	**FWHM Left (deg)**	**Crystallite Size (nm)**	**Micro Strain (%)**
25.2834	3.51970	0.4187	17.8	0.98841
37.7723	2.37975	0.6393	9.2	1.29228
38.5727	2.33220	0.3876	17.1	0.68038
48.0155	1.89328	0.3985	19.5	0.48580
53.8925	1.69986	0.6539	11.7	0.72620
55.0374	1.66718	0.4336	17.6	0.47451
62.6063	1.48258	0.8014	9.3	0.80082
68.7625	1.36409	0.6569	10.9	0.62375
70.2629	1.33859	0.4972	16.3	0.41044
75.0628	1.26445	0.7445	8.9	0.71267
82.7230	1.16569	1.0303	10.8	0.54155
			13.55	**0.70334**
1 mL				
2θ (deg)	**d-spacing (Å)**	**FWHM Left (deg)**	**Crystallite Size (nm)**	**Micro Strain (%)**
25.2735	3.52106	0.4172	18.1	0.97116
36.9304	2.43205	0.6559	13.8	0.88019
37.7917	2.37858	0.6289	13.5	0.88357
38.5615	2.33285	0.5462	16.6	0.70301
48.0131	1.89337	0.4173	19.1	0.49505
53.8941	1.69981	0.6440	12.1	0.70371
55.0362	1.66721	0.4367	17.5	0.47575
62.6035	1.48264	0.7935	9.6	0.76978
68.7263	1.36472	0.6532	11.8	0.57628
70.2667	1.33853	0.5550	14.6	0.45988
75.0738	1.26429	0.7048	9.1	0.69345
82.7361	1.16554	0.9740	8.9	0.65339
94.6146	1.04802	1.5774	6.7	0.77761
			13.18	**0.65377**

2 mL				
2θ (deg)	d-spacing (Å)	FWHM Left (deg)	Crystallite Size (nm)	Micro Strain (%)
25.1466	3.53854	0.4283	17.7	0.99734
27.2800	3.26646	0.4406	15.9	1.02667
35.9330	2.49723	0.3456	22.8	0.54686
37.6731	2.38579	0.8776	5.4	2.20809
41.1075	2.19405	0.3508	21.7	0.50491
43.8429	2.06329	0.5673	13.0	0.79545
47.8876	1.89803	0.3959	18.9	0.50103
54.1098	1.69354	0.8016	8.9	0.95158
54.9514	1.66958	0.3800	24.7	0.33733
56.4886	1.62774	0.4395	17.6	0.46269
62.5461	1.48386	0.6873	9.9	0.75112
63.9862	1.45390	0.3490	23.4	0.31087
68.7909	1.36360	0.6599	11.0	0.62222
69.9537	1.34375	0.8443	12.0	0.55902
74.9809	1.26563	0.9734	7.2	0.87294
82.5061	1.16821	1.1333	9.8	0.59823
89.4831	1.09431	0.4025	30.5	0.17966
			15.90	**0.55879**

